



THE VORTEX ACTIVATION METHOD OF REAGENT WATER TREATMENT

Nikolay LAGUNTSOV, Vissarion KIM, Petr KRASNOV,
Yury NESHCHIMENKO, Maxim BORISENKO,
Anatoly ODINTSOV, Andrey FARTUNIN

JSC "Aquaservice", 31, Kashirskoe Street., 115409 Moscow, Russia
e-mail: aquaserv@mail.ru

ABSTRACT

The experimental study on vortex activation method of reagent water purification from oil products and suspension particles using the alumosilicon flocculant-coagulant (ASFC) was made. The numerical model of water purification was suggested according to Smoluhovsky theory of coagulation kinetics.

Keywords: Coagulation, Flocculation, Water purification, Oil products, Suspension particles

INTRODUCTION

The intensification of aggregative processes under reagent water treatment allows to decrease the treatment time and to increase the quality of water purification from oil products and suspension particles. The vortex method of aggregative processes activation under water purification from oil products and suspension particles is described in this paper.

The aim of this work is to investigate the process of water purification from oil products by using a new generation reagent alumosilicon flocculant-coagulant (ASFC), where the flocculant-coagulant functions are combined.

The raw material for the reagent ASFC production is an "aluminous" nepheline concentrate and sulphuric acid of low arsenic concentration. Nepheline concentrate is a by-product of apatite production. Main components of nepheline are: silicon oxide SiO_2 of flocculating properties,

and alumina Al_2O_3 of coagulation properties. There are other oxides Fe_2O_3 , Na_2O , K_2O at low concentration, but they do not influence coagulation and could be ignored. When nepheline concentrate interacts with sulphuric acid, a mixture of alumoquartz with hydrated silicic acid is formed: $(\text{Na},\text{K})_2\text{SO}_4\text{Al}_2(\text{SO}_4)_3\text{mH}_2\text{O} + 2\text{SiO}_2\text{nH}_2\text{O}$. The filtrate of this solution was named ASFC. Hydrolysis processes occur rapidly in neutral and alkaline media. Thus, this kind of solution is kept in a subacid medium. When a reagent is added to the polluted water, the process of aluminium ions hydrolysis begins. Then, the flocculation process is accomplished and finally aluminium and silicon hydrocomplexes of flocculating properties are formed. Therefore, the ASFC reagent combines coagulant and flocculant functions.

The mechanism of ASFC operation is based on the coagulating action of aluminium ions and subsequent aggregation of colloidal particles by "flocculation bonds" of polysilicon acids. Chain-length distribution of polysilicon acids depends on fluctuations in silicic acid concentration and pH-level in the liquid volume phase that influence on the polycondensation synthesis of silica.

The respective experimental results and an analytical model of the purification process are presented and discussed.

EXPERIMENTAL

Under vortex method of activation (Fig. 1.) the flow of fluid phase is being cast from the center to periphery. Braking of the liquid against the wall leads to increasing the pressure, which is being dependent on the rotors rotation speed as well as on its size and geometry.

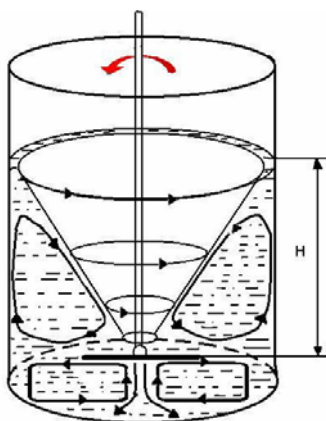


Fig. 1. The scheme of vortex activation process.

As a result, vortex circulation flow arises i.e. water located along the wall above the rotor goes up, and the water located along the axis of the rotor

goes down. A surface of their contact takes the shape of a vortex, which sucks some more air intensively. During the residence time of water in the reaction chamber, particles of admixture make frequent rotary movements. Simulation of suspension particles and oil products in water was carried out with the model clay (50-200 mg/L) and organic substances (15-30 mg/L). The vortex chambers of circular or rectangular cross section with a diameter or width up to 9 cm and height up to 15 cm were used. The hydrodynamic regime depends on the rotor design, the depth of its immersion, the gap between a rotor and a chamber wall, and others. The hydrodynamic characteristics of the rotor are listed in Table 1. Obviously, the flow is turbulent in all cases.

The concentration of volatile admixtures was determined by a gas chromatograph, and low volatile ones (spindle oil) - by a differential photocolorimeter. At the same time the oil was extracted from water with carbon tetrachloride. The photocolorimeter scale was linear in the range from 1.0 to 50.0 mg/L. For example, the calibration of photocolorimeter with low oil concentration is shown in Table 2. The threshold sensitivity of the device is 0.05 mg/L.

Table 1. The hydrodynamic characteristics one of the rotor variants: n – rpm, d_r – effective diameter of a rotor, $V_r = \pi d_r n$, $Re = V_r D_0 / \nu$, D_0 – diameter of a chamber, $V_0 = \pi d_0 n$, d_0 – diameter of a rotors shaft

n , rpm	V_r , m/s	$Re, 10^4$	H , mm	d_0 , m	V_0 , m/s
500	1.3083	3.270833	2 ±1	0.008	0.21
1000	2.6167	6.541667	4 ±1	0.01	0.52
2000	5.2333	13.08333	29 ±3	0.01	1.05
3000	7.85	19.625	40 ±6	0.01	1.57
4000	10.467	26.16667	52 ±10	0.012	2.51
5000	13.083	32.70833	95 ±15	0.012	3.14

Table 2. The results of photocolorimeter calibration

quantity of oil (mg/L)	Signal of KN-2 (units)	fractional accuracy, %
0.4	5.6	18
0.8	14	10
2.4	50.1	10
4	81.4	3

The process of purification was controlled by the turbidimetric method. The dispersed emulsion mixture was analyzed using an optical

1 μm -resolution-microscope. It is worth noticing that a sharp oil drops image could not be obtained, in contrast to clay granules. An approximate drop size in the vortex field varies from 2 to 10 μm (effective diameters). Additionally, the big 1-2 mm marks were introduced in into water and their circulation there was observed by means of a camera or visually.

The efficiency of purification from toluol is found to be low, due to its solubility in water. At that time, the efficiency of purification from oil $\alpha = c_o/c$ (where c_o and c denote oil concentrations in crude and purified water) amounts 100-300, depending on temperature. Comparative experiments showed that ASFC is about 5-7 times more efficient than $\text{Al}_2(\text{SO}_4)_3$ (at similar norms of expenditure). The α dependence on rotation speed is shown to cross maximum. Since a decrease in water purification efficiency was observed for high speed rotor frequency, it can be concluded that destruction of floccules begins under these conditions.

The initial part of the increase in $\alpha(n)$ is connected with an increase in particles collisions probability, while an inconsiderable decrease in α at $n > 3000$ rpm can be explained by shortening the contact time between interacting particles.

The dependence of purification efficiency on ASFC dose is shown in Fig.2. The rotation speed is the same in all regimes.

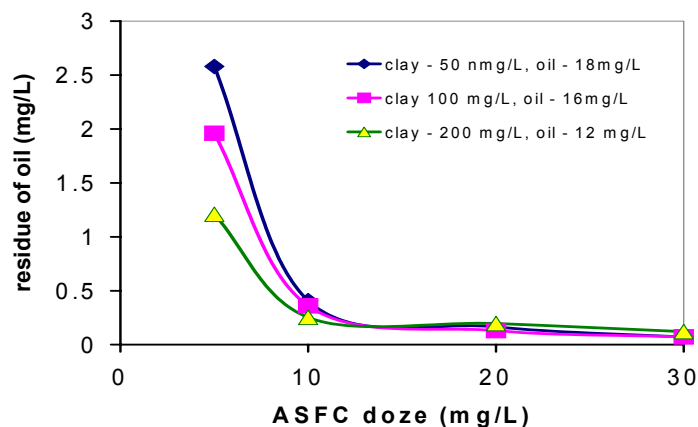


Fig. 2. The dependence of purification efficiency on ASFC doze:
 curve 1 – clay 50 mg/L, oil 18 mg/L; curve 2 – clay 100 mg/L, oil 16 mg/L;
 curve 3 – clay 200 mg/L, oil 12 mg/L.

A number of efficient collisions of particles grows when the time of water processing increases. Consequently, an increase in water purification efficiency is observed. At ASFC concentrations higher than 10 mg/L of Al_2O_3 , the purification efficiency α reaches its maximum despite the amount of suspension particles or hydrocarbons in water. At 30 °C, oil

concentration in the purified water reached the threshold value level. Temperature reduction to 8 °C caused an increase in the concentration by a factor of five-seven (under all other conditions similar). The dependence of permanent oil presence in water on the excitation time is shown in Fig. 3. Attention should be paid to the fact that oil purification does not depend on clay concentration.

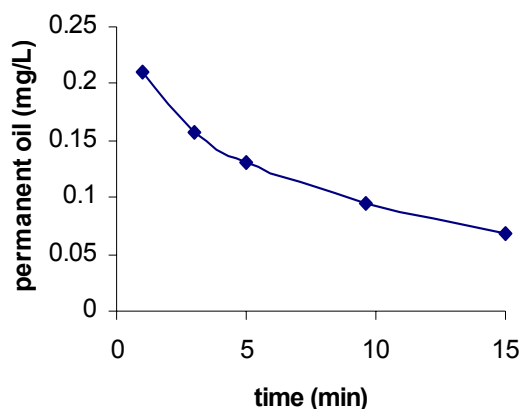


Fig. 3. The dependence of permanent oil in water on time of excitation.

ANALYTICAL MODEL

Obviously, at $n \geq 2000$ rpm and $Re > 10^5$ the flow is turbulent. The turbulent pulsations appear in the gap between the rotating disk and the frame. The additional turbulization formed by the perturbations of the free funnel-shaped surface. This suggests to assume that Kolmogorovs [4] advanced turbulence regime is being realized in the chamber. In this theory, the turbulent flow is considered as a result of an imposition of the spectrum of continuous pulsations of different scales (even the very small) on the main flow speed. As a result, intense mixing takes place and favorable conditions for rapid coagulation predicted by Smoluhovsky [3] are established. It is supposed that only collisions between two particles take place and the pollutant is monodispersed. Then, a change in the number of particles is described by Eq. (1):

$$-\frac{dn}{dt} = K \cdot n^2 \quad (1)$$

where $K = 8\pi rD$ is defined as in the paper [3], D – denotes diffusion constant of single particles. The Smoluhovsky method was developed in the theory of turbulent coagulation by Levich [5]. It is supposed that admixture particles are completely carried away by the liquid flow. The speed pulsations of $\lambda \sim R$ scale are responsible for coagulation, where R denotes instantaneous radius of the particles. At the same time, the condition that $\lambda_0 > \lambda$ must be fulfilled, where λ_0 is the inner scale of turbulization, that equals:

$$\lambda_0 \approx L / \text{Re}^{3/4} \quad (2)$$

where L – the character measure of macropulsations. Under these conditions, the turbulent diffusion coefficient is defined as

$$D_{turb} = \beta \sqrt{\varepsilon / \nu} \cdot \lambda^2 \quad (3)$$

where ε is the dissipation of energy per unit of time, divided by mass unit.

$$\varepsilon \approx \frac{\Delta v^3}{L} \quad (4)$$

In Eq. (4) Δv denotes characteristic flow speed. The value L is defined by the level of water content. β value was defined experimentally [4]. As $\lambda \sim R$, we finally obtain:

$$D_{turb} = \beta \sqrt{\varepsilon / \nu} \cdot R^2 \quad (5)$$

The effective diffusion constant is:

$$D_0 = D_{turb} + D$$

with D denoting the Brownian diffusion constant [5].

$$D = \frac{KT}{3\pi\mu r}$$

where μ - dynamic viscosity, $T=22$ °C, $r=5$ μm , $D \sim 6.9 \cdot 10^{-13}$ m^2/s . In the rapid coagulation regime, the diffusion particles transportation is defined by D_0 value. If the coagulation radius R satisfies the inequality $D_{turb} > D$, the Brownian diffusion can be ignored. The critical size of particles, for $D_{turb} \sim D$, ranges from 5 to 10 μm [5], or 1.6 – 4.6 μm [8]. However, these data do not take into account interaction of particles with the ASFC.

When the experimental data are considered, the purification process looks in the following way: upon the ASFC reagent introducing into water, its rapid and uniform distribution throughout the entire water bulk takes place along with its aqutation. Hydrolysis products cover surface of emulsion drops, thereby providing its enlargement and forming of floccules. It is significant that coagulation and flocculation processes of oil drops are different from analogous processes involving solid particles. It is connected with low oil permittivity, that's why the electrical potential in the boundary water-oil occurs mainly in the oil phase [6]. Besides, the influence of double layers on the opposite drops poles (borders) also lowers the potential in the outphase. Because of that, drops stability decreases. According to Kruyt's theory [6], the sorption of small hydrophilic particles on the drop surface increases stability of the drops due to an increase in the repulsion potential.

The aggregation process is conditionally divided into three stages:

1. Coagulation (rapid coagulation)
2. Flocculation - the initial phase (interaction between particles which were generated in the coagulation stage and flocculant particles).
3. Flocculation - the final phase (interaction between particles which generated in the second stage).

Each stage is characterized by different time. The results below

correspond with the calculation of one of the regimes with the rotor frequency 3000 rpm, and temperature ~ 22 °C. The initial clay concentration was 20 mg/L, drops size – 4 μm. With these values, the initial density of n_0 particles was defined.

It is considered, that the concentration of flocculant is defined by SiO₂ concentration in relation to Al₂O₃ in ASFC reagent. It was experimentally found that the size of flocculant particles is about 14-20 μm. The initial number of flocculant particles is n_{10} in a unit of liquid volume. This value is used when calculating the second step of flocculation. It is assumed that the flocculant does not take part in the first stage of adhesion. While calculating we assumed that the medium is monodisperse and the particles are of the spherical shape. Moreover, the presence of air bubbles in water is not taken into account.

In our case, in Smoluhovsky [3] equation $K = 8\pi r D_0$. The number of particles in the purification process changes according to Eq. (6):

$$n = \frac{n_0}{1 + \frac{t}{\tau}} \tag{6}$$

The period of coagulation τ is:

$$\tau = \frac{1}{K \cdot n_0} \tag{7}$$

r - initial, average radius of a particle; it was evaluated from the microfilming results, n_0 – initial number of polluted particles is also known. Considering that $L = 1.1 \times 10^{-1}$ m (level of water in chamber) and:

$$\lambda_0 \approx \frac{11}{(2.4 \times 10^5)^{3/4}} \text{ i.e. } \lambda_0 \approx 10^{-5} \text{ m for } R = 4 \text{ } \mu\text{m,}$$

the change in average speed is $\omega R/2 = 2.25$ m/s. Therefore, the diffusion constant is:

$$D_{urb} \approx (2.5 \times 10^2)^{3/2} \sqrt{\frac{1}{10^{-2} \times 20}} \cdot (10^{-3})^2 \text{ i.e. } D_{urb} \approx 7.5 \times 10^{-3} \text{ m}^2/\text{s}$$

Supposing that $D_0 = D_{neh}$ $n_0 = 6.7 \times 10^5$, the value τ is defined. According to our estimates, the period of coagulation $\tau \sim 0.02$ s. Thus, the first stage proceeds very quickly. After this the number of particles can be calculated using the following formula

$$n_i = n_0 \frac{\left(\frac{t}{\tau}\right)^{i-1}}{\left(1 + \frac{t}{\tau}\right)^{i+1}} \tag{8}$$

When the size of particles increases, repulsive force between them increase, too. As it is proportional to radius, attracting force does not change. Thus, among interactions particles of the size order range 5-7 (by

Smoluhovsky terminology), the probability of adhesion tends to zero. The density of the 7th order particles reaches its maximum value in the moment of time $t \approx 3\tau$. As the result of coagulation, the particles achieve to critical size and further increasing size of particles dues to flocculation. Thus, the first stage is finished when the size of particles, appearing in coagulation process, is about 10-14 μm , and the number of particles is n_{10} . The time of stage duration is about 3-5 τ , then it is necessary to consider flocculating processes.

The first stage proceeds very quickly. However, there was an assumption in calculation, that the reagent is introduced instantly. In the real time, the duration of the first stage will depend on the rate of introducing ASFC into liquid and on mixing intensity.

Now, we should discuss the first stage of flocculation. For this purpose, we choose the central flocculant particle and define flow of coagulating particles. There are particles enough big in the process ($2r \geq \lambda_0$), i.e., effective only in α_1 collision. According to Smoluhovsky, change in the number of coagulating particles can be defined as follows:

$$-\frac{dn_1}{dt} = K_{1f} \cdot n_1 \cdot n^0 \quad (9)$$

where n_1 - number of coagulating particles in the unit volume, n^0 – density of flocculant particles, K_{1f} – probability of collision, that can be defined as ([3]):

$$K_{1f} = 2 \cdot [4 + (\sqrt{r_1/r_2} - \sqrt{r_2/r_1})^2] DR \cdot W_f \quad (10)$$

where r_1 and r_2 - radii of particles, R – distance between particles. Probability of flocculation can be defined by formula:

$$W_f = \exp(-s_1/s_0) \cdot (2 - \exp(-s_2/s_0))^{s_1/s_2} - \exp(-2s_1/s_0) \quad (11)$$

Where s_0 - square of particles surface in one associate, s_1 - square of the contact area during particles collision, s_2 -square of cross-section of associate flocculant molecules. The characteristic time of the first flocculation stage is:

$$\tau_{1f} = \frac{1}{K_{1f} \cdot n^0 \cdot \alpha_1} \quad (12)$$

Taking for calculations $\alpha_1 = 0.3$, one can obtain:

$$n_1 = n_{10} \exp(-K_{1f} n^0 t) \quad (13)$$

Under these conditions $K_{1f} = 8.7 \times 10^{-5} \text{ cm}^3/\text{s}$, $n^0 = 5 \times 10^2 \text{ cm}^{-3}$, $n_{10} = 1.5 \times 10^4 \text{ cm}^{-3}$, $\tau_{1f} = 80 \text{ s}$, and:

$$\frac{n_1}{n_{10}} = \exp(-0.0125 \cdot t) \quad (14)$$

The moment of finishing time of the first stage of flocculation was estimated similarly to the coagulation stage. The size of the particles obtained is about 40-50 μm.

It may be expected, that in the second stage the particles, which appeared in the first stage, are of the same size. The density of particles vs. time derivative is described by Eq. (15):

$$-\frac{dn_2}{dt} = \alpha_2 \cdot K_{2f} \cdot n_2^2 \tag{15}$$

The coefficient α_2 takes into account effective collisions. After the integration we can define the dependence of a number of particles on time:

$$n_2 = \frac{n_2^0}{1 + \alpha_2 K_{2f} n_2^0 t} \tag{16}$$

where n_2^0 - the initial number of particles in the second stage,

$$K_{2f} = 8\pi R D_0 \cdot W_f \tag{17}$$

Consequently, the characteristic time of the second flocculation stage is:

$$\tau_{2f} = \frac{1}{\alpha_2 \cdot k_{2f} n_2^0} \tag{18}$$

$K_{2f} = 8 \times 3.14 \times 42 \times 10^{-4} \times 7.5 \times 10^{-3} \times 0.24 = 1.9 \times 10^{-4}$, $n_2^0 \approx 500 \text{ cm}^{-3}$, $\alpha_2 = 0.05$, $\tau_{2f} \approx 480 \text{ s}$. The number of primary particles decrease according to Eq. (16). After time $t \approx 480 \text{ s}$, the average number of particles $n^* \approx 250 \text{ cm}^{-3}$.

We should note that the shape of big floccules is different from the spherical one. Besides, while the size of particles increases, the density decreases. If the average statistical distance between the particles is higher than a characteristic scale of turbulent pulsations (that are responsible for the processes of adhesion) the theory of rapid coagulation does not work.

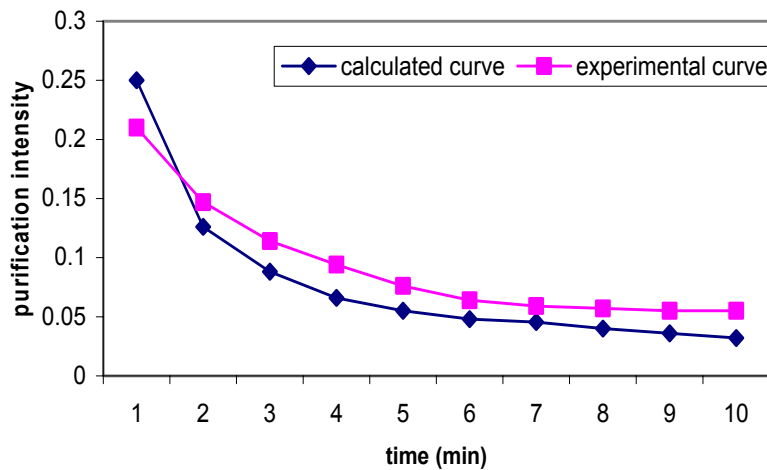


Fig. 4. The dependences of purifications efficiency α on time of mixing. 1 – calculated curve, 2 – experimental curve, $n = 3000 \text{ rpm}$.

The values of $n_0(t=0), n_{10}(t_1), n_2^0(t_2), n^*(t_3)$ have been used to plot an approximating function $n(t)$ presented in Fig. 4. as the curve 1 in the dimensionless units. The experimental results are shown as the curve 2.

These calculations correspond with monodisperse systems. However, real admixtures are polydisperse and coagulation occurs faster, i.e., big particles assist small particles in coagulation ([6],[7]). Nevertheless, Fig. 4. show that lowering the coefficients of flocculant processes α_1 and α_2 results in good agreement between experimental and calculated results.

CONCLUSION

A new scheme of coagulation and flocculation intensification as based on using vortex mode of the flow was developed. Under these conditions an effective purification from some marginally soluble oil-products was carried out. At the same time, this method does not affect dissolved admixtures (toluol).

Thus, the vortex activation method provides efficient purification of water from oil. The fine dispersed emulsion is formed in the vortex field. The products of the reagent (ASFC) hydrolysis are collected on the surfaces of the oil drops, associates of which fall out in sediment.

An attempt to describe the experimental results, (photocolorimetry, turbidimetry and microfilming) by using the theory of rapid coagulation and an approximate model of vortex activation of coagulation and flocculation processes was performed.

It is reasonable to use the vortex scheme of water purification at the final stage of purification, i.e. when concentrations are lower than 10-20 mg/L.

In the context of the presented model, the processes of coagulation and flocculation are characterized by temporary parameters $\tau, \tau_{1f}, \tau_{2f}$ that functionally depend on the main operation parameters. Therefore, a role of different factors on the purification process can be estimated.

REFERENCES

- [1] V.E. Kim, N.I. Laguntsov, B.S. Lisujk, V.F. Karpukhin. *The method of water purification*, Patent №2114787. B.I. №19. 1998.
- [2] M. Smoluhovsky, *Physikalische Zeitschrift*, 1913, 17, 586.
- [3] M. Smoluhovsky, *Zeitschrift für Physikalische Chemie*, 1917, 92, 120.
- [4] L.D. Landau, E.M. Lifshitz. *Course of Theoretical Physics, Vol.6. Fluid Mechanics*, Institute of Physical Problems, USSR Academy of Sciences. (Translated by J.B. Sykes and M.J. Kearsley), Oxford.2000.
- [5] V.G. Levich, *Physicochemical hydrodynamics*, Prentice-Hall, 1962.
- [6] H.R. Kruyt, *Colloid Science*, vol. 1, Elsevier Publishing Company, 1982.
- [7] H. Mueller, *Kollo. Z.*, 1923, 32, 29.
- [8] N. Tambo, *Mem. Fac. Engng. Hokkaido Univ.*, 1965, 11, 585.